

Early Changes in Pancreatic Acinar Cell Calcium Signaling after Pancreatic Duct Obstruction*

Received for publication, July 24, 2002, and in revised form, December 19, 2002
Published, JBC Papers in Press, January 8, 2002, DOI 10.1074/jbc.M207454200

Frank Ch. Mooren^{‡§¶}, Verena Hlouschek^{¶¶}, Till Finkes[‡], Stefan Turi[‡], Ina Alexandra Weber[‡],
Jaipaul Singh^{||}, Wolfram Domschke[‡], Jürgen Schnekenburger[‡], Burkhard Krüger^{**},
and Markus M. Lerch[‡] ^{‡‡}

From the [‡]Medizinische Klinik B and [§]Institut für Sportmedizin, Westfälische Wilhelms-Universität, 48129 Münster, Germany, ^{||}Cell Communication Group, Department of Applied Biology, University of Central Lancashire, Preston PR12HE, United Kingdom, and ^{**}Division of Medical Biology, Department of Pathology, University of Rostock, 18057 Rostock, Germany

Intracellular Ca^{2+} -changes not only participate in important signaling pathways but have also been implicated in a number of disease states including acute pancreatitis. To investigate the underlying mechanisms in an experimental model mimicking human gallstone-induced pancreatitis, we ligated the pancreatic duct of Sprague-Dawley rats and NMRI mice for up to 6 h and studied intrapancreatic changes including the dynamics of $[\text{Ca}^{2+}]_i$ in isolated acini. In contrast to bile duct ligation, pancreatic duct obstruction induced intrapancreatic trypsinogen activation, leukocytosis, hyperamylasemia, and pancreatic edema and increased lung myeloperoxidase activity. Although resting $[\text{Ca}^{2+}]_i$ in isolated acini rose by 45% to 205 ± 7 nmol, the acetylcholine- and cholecystokinin (CCK)-stimulated calcium peaks as well as the amylase secretion declined, but neither the $[\text{Ca}^{2+}]_i$ -signaling pattern nor the amylase output in response to the Ca^{2+} -ATPase inhibitor thapsigargin nor the secretin-stimulated amylase release were impaired by pancreatic duct ligation. On the single cell level pancreatic duct ligation reduced the percentage of cells in which submaximal secretagogue stimulation was followed by a physiological response (*i.e.* Ca^{2+} oscillations) and increased the percentage of cells with a pathological response (*i.e.* peak plateau or absent Ca^{2+} signal). Moreover, it reduced the frequency and amplitude of Ca^{2+} oscillation as well as the capacitative Ca^{2+} influx in response to secretagogue stimulation. Serum pancreatic enzyme elevation as well as trypsinogen activation was significantly reduced by pretreatment of animals with the calcium chelator BAPTA-AM. These experiments suggest that pancreatic duct obstruction rapidly changes the physiological response of the exocrine pancreas to a Ca^{2+} -signaling pattern that has been associated with premature digestive enzyme activation and the onset of pancreatitis, both of which can be prevented by administration of an intracellular calcium chelator.

Alterations in intracellular calcium signaling have previously been reported from an experimental animal model of acute pancreatitis that employs supramaximal secretagogue stimulation for the disease induction (1). Moreover, the spatial and temporal distribution of intracellular calcium signals in response to either physiological or pathological stimuli has been found to be directly related to premature digestive enzyme activation in the pancreas and to acinar cell injury (2–5). Intracellular activation of trypsinogen on the other hand can be completely prevented with agents that interfere with either the uptake of calcium, the maintenance of a calcium gradient across the plasma membrane, or the rapid release of calcium from apical intracellular stores (4, 6). All of these studies indicate clearly that the spatial and temporal distribution of intracellular calcium signals plays a critical role in the early cellular events that precede the onset of pancreatitis. The mechanism, however, that was used to induce acinar cell injury in these studies or in response to which intracellular calcium changes were characterized, supramaximal secretagogue stimulation, is not necessarily an event that is generally involved in the pathogenesis of clinical pancreatitis.

In many parts of the world the most common etiological factor associated with acute pancreatitis is gallstone disease. Experimental (7) as well as clinical studies (8, 9) suggest that the onset of gallstone-induced pancreatitis requires migration of the offending stone through the biliary tract and its impaction at the duodenal papilla. Here, at the junction of the common bile duct and the pancreatic duct, the stone can impair the flow of pancreatic secretion or lead to a complete blockage of the pancreatic duct. It is now generally accepted that this impairment of pancreatic secretion (7, 10, 11), rather than a potential reflux of bile into the pancreas (13), represents the critical pathophysiological event for the development of gallstone-induced pancreatitis. To investigate whether this clinically relevant mechanism for the onset of pancreatitis is, in analogy to the secretagogue-induced animal models, associated with intracellular calcium changes and premature protease activation, we ligated the pancreatic duct of laboratory animals for up to 6 h. The results from our experiments indicate that pancreatic duct obstruction is indeed followed by rapid changes in the response of acinar cells to secretory stimuli, leads to complex pathological alterations in the intracellular Ca^{2+} -signaling pattern, and induces premature digestive enzyme activation. *In vivo* administration of an intracellular Ca^{2+} chelator on the other hand can largely prevent hyperamylasemia, hyperlipasemia, and intrapancreatic trypsinogen activation.

* This work was supported by Interdisziplinäres Zentrum für Klinische Forschung Münster Grants H3 and D21 and Deutsche Forschungsgemeinschaft Grants KR 1274/2-2, Le 625/5-2, and SFB 293 B7. The costs of publication of this article were defrayed in part by the payment of page charges. This article must therefore be hereby marked "advertisement" in accordance with 18 U.S.C. Section 1734 solely to indicate this fact.

[¶] These authors were equal contributors.

^{‡‡} To whom correspondence should be addressed: Dept. of Medicine B, Westfälische Wilhelms-Universität, Albert-Schweitzer-Str. 33, 48129 Münster, Germany. Tel.: 49-251-8347559; Fax.: 49-251-8349504; E-mail: markus.lerch@uni-muenster.de.

EXPERIMENTAL PROCEDURES

Materials—Fura-2-acetoxymethyl ester (AM) was from Molecular Probes (Eugene, Oregon). Cell-Tak was obtained from Collaborative Research Inc., Bedford, MA. Rhodamine-labeled phalloidin was obtained from Molecular Probes (Junction City, OR). All other reagents were of the highest purity available and were purchased from Sigma unless indicated otherwise.

Surgical Procedure—All animal experiments were approved by and conducted under the guidelines of the Animal Use and Welfare Committee of the University of Münster. Male Sprague-Dawley rats weighing between 250 and 350 g and adult male NMRI mice weighing between 30 and 35 g (both species from Charles River, Sulzfeld, Germany) were kept in Nalgene shoebox cages in a 12-h/12-h light/dark cycle with unlimited access to standard chow and water. All animals were adjusted to laboratory conditions over the course of 1 week before the experiments. After a 12-h fast with free access to drinking water and after anesthesia with sodium pentobarbital (72 mg/kg of body weight), the abdomen was opened, and the pancreas was exposed. Above the head of the pancreas the common bile duct was ligated in all animals (bile duct controls and treatment group), and subsequently, the main pancreatic duct was ligated without affecting the splenic vessels in the treatment group. In addition to sham-operated controls for most experiments (laparotomy only) a bile duct-ligated control group was used for several reasons as follows. (a) Bile duct ligation alone is known to raise circulating cholecystokinin levels in the blood and could, by itself, exert a stimulatory effect on the pancreas (14). (b) It has been suggested that bile duct obstruction could be a confounding or aggravating factor for the events involved in pancreatic duct obstruction-induced pancreatitis (15, 16). (c) Ligation of the pancreatic duct system in mice without compromising the unimpeded flow of bile is technically more prone to surgical complications than ligation of both ducts and the latter is a more likely to reflect the situation that arises when a gallstone is impacted at the papilla. At time intervals of up to 6 h the anesthetized animals were killed by cervical dislocation, venous blood was collected from the right ventricle, and the pancreas was rapidly removed for either morphology, enzyme activity measurements, or fresh acinar cell isolation. In a series of experiments that were performed to modify the pathological calcium-signaling pattern in pancreatic acinar cells that was associated with pancreatic duct ligation we used the calcium chelator BAPTA-AM in *in vivo* experiments. BAPTA-AM was administered intraperitoneally in mice (10 μ g/kg of body weight in 180 μ l of propylene glycol as a solvent) by 2 single injections at 30 min before the operation and at the time of laparotomy. Controls received only propylene glycol vehicle intraperitoneally. Serum activities of amylase and lipase as well as trypsinogen activation peptide in the pancreas were measured 4 h after pancreatic duct ligation. After sacrifice pancreatic tissue was either fixed for morphological studies, snap-frozen for the assays outlined below, or desiccated for 12 h at 160 °C to determine the dry/wet weight ratio as an indicator of pancreatic edema formation.

Cell Isolation Procedures—The reason for using rats as well as mice for our studies was 2-fold. One reason was to test our hypotheses in different species of laboratory animals, and the second was the observation that rat pancreatic acini preparations permit a greater yield, whereas mouse pancreatic acinar cells are better suited for single cell microfluorometry. In the following we briefly outline the somewhat different protocols for acinar cell preparations from mouse and rat pancreas. The rat pancreas was immediately transferred to iced medium (preoxygenated for 10 min) composed of modified Krebs-Ringer-HEPES buffer containing NaCl (130 mM), KCl (5 mM), HEPES (20 mM), KH_2PO_4 (1.2 mM), MgSO_4 (2 mM), glucose (10 mM), CaCl_2 (1 mM), soybean trypsin inhibitor (0.1 mg/ml), bovine serum albumin, 0.2% (w/v) at pH 7.4. The tissue was rapidly minced with scissors, and acinar cells were dissociated by incubation in calcium-free medium containing collagenase type V (268 units/ml) for 25 min at 37 °C in a shaking water bath (17, 18). The collagenase solution was discarded, and the cell suspension was washed 3 times with calcium-free medium, filtered through a nylon mesh, and centrifuged with medium containing 5% bovine serum albumin. Finally the cell suspension was centrifuged and resuspended in Krebs-Ringer-HEPES medium.

For single cell studies mouse pancreas was rapidly removed, minced into small pieces on ice, and placed into buffer (pH 7.4) containing NaCl (130 mM), KCl (5 mM), HEPES (10 mM), KH_2PO_4 (1.2 mM), CaCl_2 (1 mM), MgSO_4 (1 mM), glucose (10 mM), and collagenase (100 units/ml Type V). After 10 min of incubation at 37 °C under continuous shaking (120 cycles/min) the digested tissue was washed 3 times in 10 ml of Krebs-Ringer-HEPES buffer without collagenase and again shaken 10 times

to dissociate acini. Acini were then filtered through muslin gauze, centrifuged at 400 rpm for 3 min, and washed twice more in buffer containing 4% bovine serum albumin. After the second wash, acini were suspended in 8 ml of Krebs-Ringer-HEPES buffer containing soybean trypsin inhibitor (0.1 mg/ml) and bovine serum albumin (0.2% w/v). A stock suspension of acini was kept on ice for up to 4 h without significant reduction in cell viability (>95%) as assessed by trypan blue exclusion.

Enzyme Activity and Activation Measurements—Pancreatic acini were transferred to 5-ml vials with aliquots of Krebs-Ringer-HEPES medium and incubated with secretagogue at 37 °C and constantly agitated for 5 min. After centrifugation at $50 \times g$ for 5 min, amylase activity was measured in the supernatant by on-line fluorometry using amylopectin anthranilate as a substrate (19, 20). Amylase measurements were expressed as units/ml supernatant/100 mg of acinar cells. The values obtained were calibrated against an α -amylase activity standard. To determine the extend of premature and intracellular trypsinogen activation, a parameter that has been found to closely parallel the severity of pancreatitis (21), we measured the generation and excretion of trypsinogen activation peptide (TAP)¹ in urine and pancreatic tissue of mice after pancreatic duct ligation using a standardized enzyme-linked immunosorbent assay (Biotrin, Dublin, Ireland) as previously reported (22, 23). Myeloperoxidase activity in lung tissue was determined as previously described in detail (23) using purified myeloperoxidase (Calbiochem) as a standard.

Acinar Cell Morphology—After removal of the pancreas of sham operated, bile duct-ligated and pancreatic duct-ligated animals small tissue sections of 2 mm were immediately fixed in an iced solution of 2% formaldehyde, 2% glutaraldehyde, embedded in Epon, post-fixed, and contrasted with osmium, uranyl, and lead. Semithin section were studied by light microscopy and thin sections evaluated on a Philips EM10 electron microscope as previously reported (24). To study the acinar cell microfilament network after pancreatic duct ligation, tissue was snap-frozen in liquid nitrogen, and 5- μ m cryosections were placed on poly-L-lysine-coated coverslips, fixed with 4% formaldehyde in PBS, and incubated with rhodamine-labeled phalloidin for 20 min in the dark. The micrographs shown in Fig. 3 were taken by electron microscopy or fluorescence microscopy and are representative for four or more individual experiments.

Measurements of $[\text{Ca}^{2+}]_i$ —Intracellular Ca^{2+} concentrations were determined using the calcium-sensitive fluorescent dye fura-2. For acinar cell suspension experiments rat acinar cells were loaded with 1 μ M fura-2/AM for 25 min at room temperature. After washing the cells were incubated for another 20 min in Krebs-Ringer-HEPES medium to permit complete de-esterification of the probe. Measurements were performed in a PerkinElmer Life Sciences LS-50B spectrofluorimeter using excitation wavelengths of 340 and 380 nm, and emitted light was collected at 510 nm. After each experiment the signals were calibrated according to Grynkiewicz *et al.* (25) by incubating cells in either calcium-free medium (1 mM EGTA) or calcium-containing buffer in the presence of 100 μ M digitonin for complete permeabilization.

For microfluorometric studies of $[\text{Ca}^{2+}]_i$ dynamics mouse acini were loaded with the AM-ester or fura-2 (5 μ M) at room temperature for 20 min. Fura-2-loaded cells were plated onto glass coverslips coated with Cell-Tak (1 μ l/cm²) and kept at room temperature for 30 min before they were mounted in a perfusion chamber with an internal volume of 0.28 ml and placed on the stage of a Nikon Diaphot-TMD inverted microscope equipped with a Fluor $\times 100$ oil immersion objective. Acini were continuously perfused with medium at a flow rate of 3 ml/min at room temperature. Fluorochrome excitation (340 and 380 nm for fura-2) was achieved using a xenon lamp in series with two chopper-linked monochromators that were coupled to the microscope via fiber optics. Emitted light was collected behind a band-pass filter (509 nm for fura-2) by a photomultiplier. In unloaded controls background fluorescence was found to be negligible.

Ratios obtained from the dual excitation wavelengths probe fura-2 were converted to calcium concentrations as previously reported (25, 26) using the formula $[\text{Ca}^{2+}]_i = (R - R_{\min}) / (R_{\max} - R) \times K_d - (I_{\text{ion-free}} / I_{\text{ion-saturated}})_{380 \text{ nm}}$, in which R_{\min} and R_{\max} are the minimal and maximal ratios obtained in either ion-free or ion-saturated solutions, respectively, K_d is the dissociation constant of fura-2 for calcium, and I is the fluorescence intensity at the 380-nm wavelength of the free dye divided

¹ The abbreviations used are: TAP, trypsinogen activation peptide; Ach, acetylcholine; CCK, cholecystokinin; BAPTA-AM, acetoxymethyl ester (AM) of 1,2-bis(2-aminophenoxy)ethane-*N,N,N',N'*-tetraacetic acid.

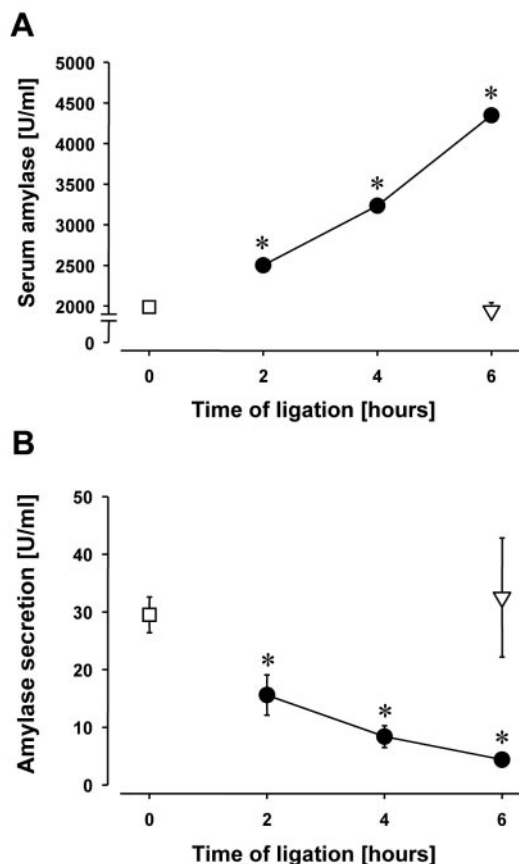


FIG. 1. Effect of pancreatic and bile duct ligation in the rat on serum amylase activity *in vivo* (A) and stimulated amylase secretion from isolated pancreatic acini (B). After surgical bile duct ligation in control animals (*open triangles*) and pancreatic duct ligation in the treatment group (*filled circles*) serum amylase activity was measured over intervals of up to 6 h (A) and compared with sham-operated animals (*open squares*). Alternatively, isolated acini were prepared by collagenase digestion (B) and stimulated with acetylcholine (10^{-7} mol liter $^{-1}$) as described under "Experimental Procedures." Although bile duct ligation alone had no effect on either serum amylase activity or stimulated amylase secretion, pancreatic duct ligation rapidly induced increased serum levels and reduced secretion of amylase from acini. Data represent means \pm S.E., and *asterisks* indicate significant differences at the 5% level compared with controls. *U*, unit(s).

by the saturated ion-dye complex. All calibration parameters were obtained in separate experiments.

Statistical Analysis—Data shown in the figures are representative of six or more individual experiments in each group and indicate the means \pm S.D. or S.E. Differences between groups were compared using Student's *t* test with Bonferroni correction where more than two groups were compared. *Asterisks* in the figures indicate statistically significant differences when the *p* values were <0.05 .

RESULTS

Acinar Cell Function and Acinar Cell Damage—In the rat bile duct ligation alone had no effect on either serum amylase activity, acinar cell damage, or the basal and secretagogue-stimulated amylase secretion (Fig. 1, A and B). Over the 6-h course of duct ligation in rats no difference between the basal amylase release from acini of bile duct-ligated (16.47 ± 3.20 units/ml/100 mg; $n = 23$) and pancreatic duct-ligated animals (14.34 ± 3.01 units/ml/100 mg; $n = 19$) was found. In contrast, the acetylcholine (*Ach*; 10^{-7} mol/liter)-induced amylase secretion from isolated acini decreased to a nadir of $\sim 16\%$ of bile duct controls, whereas serum amylase activity increased in parallel. These data indicate that acinar cell damage (Fig. 1A) and acinar cell secretory dysfunction (Fig. 1B), respectively, can already be detected as early as 2 h after pancreatic duct ligation.

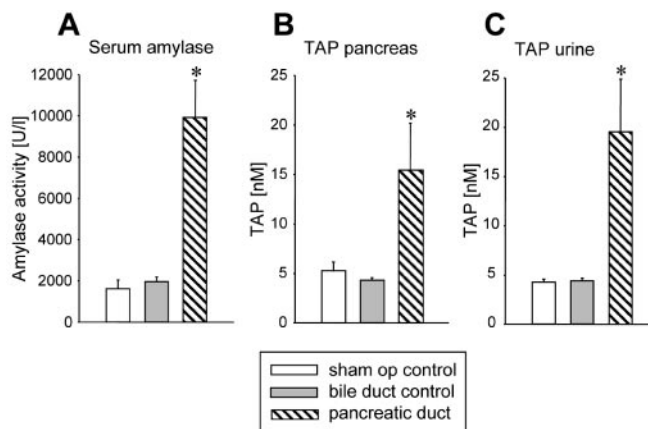


FIG. 2. Effect of pancreatic and bile duct ligation on serum amylase activity and TAP concentrations in the mouse. NMRI mice underwent either surgical bile duct ligation (*gray bars*), pancreatic duct ligation (*hatched bars*), or sham operation (*op*; *white bars*) and were sacrificed after 4 h. Serum amylase activity (A), TAP levels in pancreatic tissue homogenate (B), and urine (C) were measured as described under "Experimental Procedures." Although bile duct ligation alone had no effect on either serum amylase activity or trypsinogen activation, pancreatic duct ligation was followed by significant increases in both parameters. Data represent means \pm S.E., and *asterisks* indicate significant differences at the 5% level compared with controls. *U*, unit(s).

When we characterized pancreatic duct ligation-induced pancreatic damage in the mouse, serum amylase activity rose just as significantly as in the rat model (Fig. 2A). Moreover, a premature and intrapancreatic activation of trypsinogen could be demonstrated by increased TAP levels in pancreatic tissue and the urine of pancreatic duct-ligated mice at 4 h (Fig. 2, B and C). On ultrastructural morphology bile duct ligation alone had no effect on either pancreatic duct cell (Fig. 3A) or exocrine cell morphology (Fig. 3B). The latter preserved their characteristic structure with zymogen granules grouped at the apical pole and around the lumen. After 4 h of combined pancreatic and bile duct ligation the ducts were found to be largely distended (*arrow* in Fig. 3C), and some duct-lining cells had damaged cell membranes facing the lumen. Acinar cells on the other hand had not undergone any necrotic changes at this time; their lumen was only marginally distended (*asterisk* in Fig. 3C), and the most prominent intracellular change was a dilatation of the endoplasmic reticulum (Fig. 3D). To study the actin microfilament network, which is known to be critically involved in fusion/fission events of zymogen granule exocytosis, we used phalloidin-labeled cryosections. In untreated control animals (Fig. 3E) or animals after bile duct ligation (Fig. 3F) F-actin labeling was found at the terminal microfilament web surrounding the acinar lumen (*asterisks*) as well as along the lateral and basal membrane (*arrows*). After pancreatic duct ligation (Fig. 3G) F-actin labeling remained unchanged at the apical locations, whereas it was redistributed from the basal acinar cell membrane to the basal cytosol surrounding the nuclei (*circles* in Fig. 3G). This suggests that the apical microfilament web involved in zymogen granule fusion/fission events remains unaffected by pancreatic duct ligation.

Systemic and Inflammatory Response to Pancreatic Duct Ligation—To permit a comparison between pancreatic duct ligation in rodents with other models of experimental pancreatitis we determined a variety of parameters that are known to reflect disease severity or systemic inflammatory response. As shown in Fig. 4 and in contrast to bile duct ligation, pancreatic duct obstruction was followed by a significant increase in circulating leukocytes (Fig. 4A), pancreatic edema (Fig. 4B), and lung myeloperoxidase activity, all of which have been reported

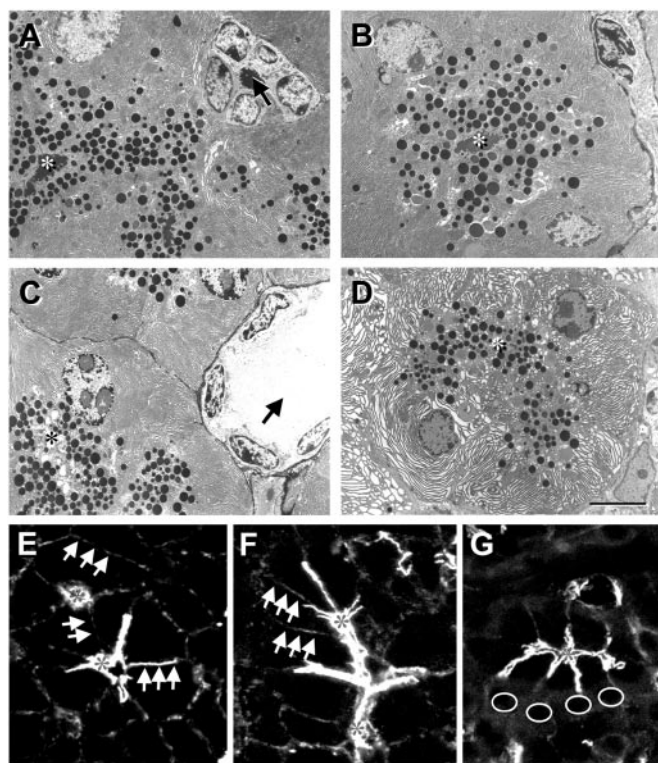


FIG. 3. Effect of pancreatic and bile duct ligation on pancreatic morphology. Plastic-embedded thin sections of mouse pancreatic tissue after surgical bile duct ligation (A and B) and pancreatic duct ligation (C and D) were contrasted with osmium, uranyl, and lead, and random fields were photographed at a standardized $\times 1800$ magnification. Images shown are representative for four or more samples from each group. Bile duct ligation alone had no discernible effect on the ultrastructural morphology of acinar cells and their luminal surface (asterisks in A and B) or on the epithelial cells lining pancreatic ducts (arrows) (arrows in C). Up to 4 h of pancreatic duct ligation led to apical formation of small vacuoles in acinar cells (C) and dilatation of the endoplasmic reticulum (D) but not to a significant distension of the acinar lumen (asterisks). The latter effect was prominent in the lumen of pancreatic ducts (arrow in C). Bars indicate $10 \mu\text{m}$. On phalloidin-labeled cryosections of pancreatic tissue F-actin was localized prominently in the apical microfilament web surrounding the acinar lumen (asterisks) as well as along the basal and lateral plasma membrane (arrows) of pancreatic acinar cells. This distribution was identical in the pancreas of sham operated (E) and bile duct-ligated (F) animals. In the pancreas, after 4 h of pancreatic duct ligation (G) the apical and lateral F-actin distribution remained unchanged, whereas that at the basal plasma membrane was greatly reduced and redistributed to the basal cytosol, where it surrounded the acinar cell nuclei (circles).

to a comparable degree in other experimental models of acute pancreatitis, including the secretagogue-induced variety (23).

Ca^{2+} Signaling after Pancreatic and Bile Duct Ligation—To study the effect of a calcium-mobilizing secretagogue on the response of acini from bile and pancreatic duct-ligated animals we stimulated them with acetylcholine (10^{-5} M). In suspensions of acini this typically resulted in a biphasic response of $[\text{Ca}^{2+}]_i$ that begins with a rapid release of Ca^{2+} from intracellular stores (peak phase) and is followed by a sustained Ca^{2+} influx (plateau phase, Fig. 5A). Because the absolute resting levels of $[\text{Ca}^{2+}]_i$ were already changed dramatically in acini from the pancreatic duct-ligated group (see Fig. 5B), we compared secretagogue-induced changes in $[\text{Ca}^{2+}]_i$ as increases over basal levels ($\Delta[\text{Ca}^{2+}]_i$) in either the peak-phase (maximum $\Delta[\text{Ca}^{2+}]_i$) or in the plateau-phase ($\Delta[\text{Ca}^{2+}]_i$ between 60 and 100 s after the peak). When we studied basal intracellular calcium concentrations in acini from control rats they were in the low nanomolar range (140 ± 5 nmol). In bile duct-ligated control animals the resting $[\text{Ca}^{2+}]_i$ was slightly decreased in comparison

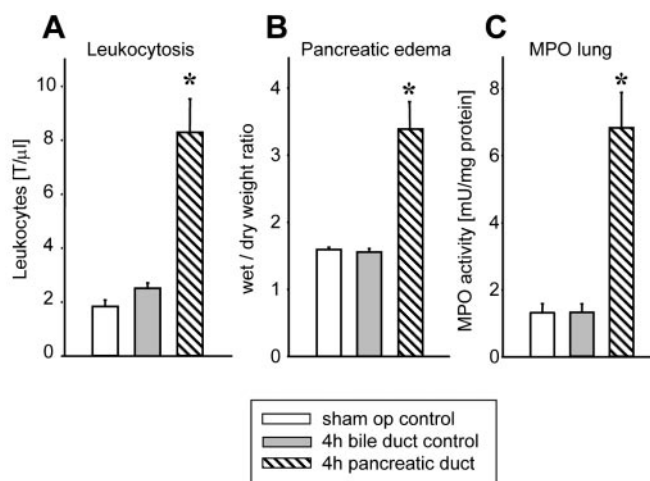


FIG. 4. Parameters of severity and inflammation. Rats underwent surgery or sham operation as described under “Experimental Procedures.” Compared with sham-operated animals (empty bars) and bile duct-ligated controls (gray bars) 4 h of pancreatic duct ligation (hatched bars) led to significant leukocytosis (A), the formation of pancreatic edema (B), and an increased myeloperoxidase (MPO) activity in the lungs (C). Data represent means \pm S.E., and asterisks indicate significant differences at the 5% level compared with sham-operated controls. *mU*, milliunit(s); *T*/ μl , thousand/microliter.

to sham-operated controls but remained constant at this level throughout the 6-h observation period (Fig. 5B). Ligation of the pancreatic duct on the other hand induced a gradual and consistent increase of resting $[\text{Ca}^{2+}]_i$ in acinar cells to a maximum of 205 ± 7 nM after 6 h (Fig. 5B).

During the rapid peak phase after acetylcholine stimulation the increase in $[\Delta\text{Ca}^{2+}]_i$ in acini from bile duct-ligated animals remained roughly in the range of control animals, whereas it decreased significantly and continuously in acini from the pancreatic duct-ligated group (Fig. 5C). The differences between the groups were even more pronounced during the subsequent plateau phase because $\Delta[\text{Ca}^{2+}]_i$ declined in acini from pancreatic duct-ligated animals and, at least in the last phase of up to 6 h, increased in the bile duct-ligated group (Fig. 5D).

When we investigated other calcium-mobilizing agents in comparison to acetylcholine we found that the response to physiological concentrations of cholecystokinin (10^{-8} M) was similarly impaired and consisted in a reduced amylase secretion by 75% (Fig. 6A) as well as an equal reduction in either the peak or the plateau $\Delta[\text{Ca}^{2+}]_i$ after stimulation (Fig. 6C). In contrast, when we used thapsigargin (10^{-6} M), an inhibitor of Ca^{2+} -ATPases that releases $[\text{Ca}^{2+}]_i$ by a different, not receptor- or G-protein-coupled mechanism, we found that the subsequent amylase secretion was unimpaired in the acini from pancreatic duct-ligated animals (Fig. 6A). This increase in $[\text{Ca}^{2+}]_i$ in response to thapsigargin, which does not follow a peak/plateau pattern (3) (these two phases are, therefore, not distinguished in Fig. 6C), was even somewhat higher in the pancreatic duct-ligated animals. When we investigated amylase secretion in response to secretin, a cAMP-mediated stimulus, we found it, in analogy to the thapsigargin experiments, not to be impaired by pancreatic duct ligation (Fig. 6B). These data indicate that the observed impairment of calcium-mediated secretion after pancreatic duct ligation affects, indeed, only calcium-mediated pathways and is not due to cellular damage in general. To further rule out that a disproportionate rate of acinar cell necrosis would account for some of the functional changes, we measured lactate dehydrogenase release from resting and stimulated acini after either bile or pancreatic duct ligation. Lactate dehydrogenase release did not exceed 1.5–2.3% of the total cellular lactate dehydrogenase in any of

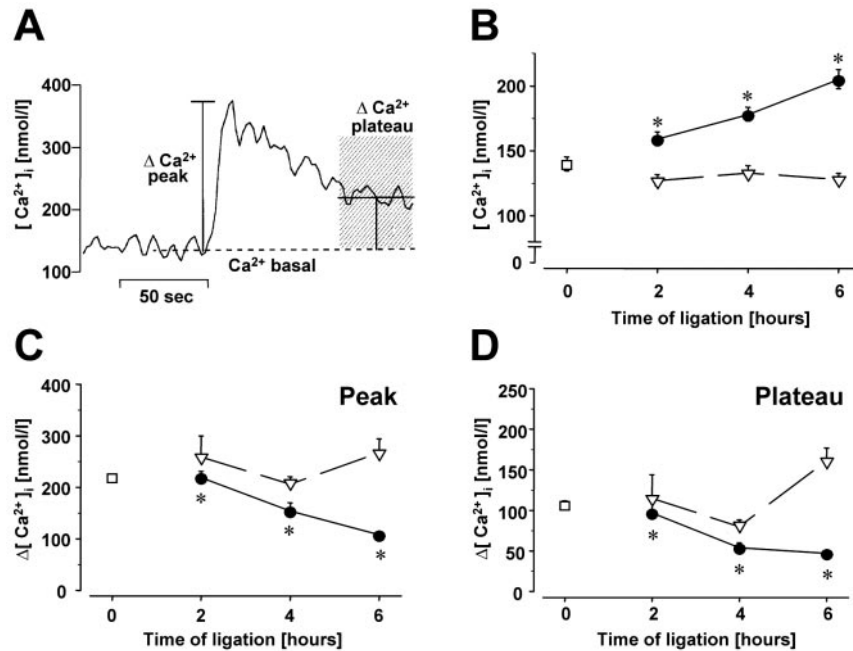


FIG. 5. **Intra-acinar cell calcium transients after pancreatic and bile duct ligation.** Isolated acini were generated from rat pancreas by collagenase digestion after animal sacrifice at intervals of up to 6 h after either surgical bile duct ligation (triangles), combined pancreatic and bile duct ligation (filled circles), or sham operation (squares). $[Ca^{2+}]_i$ was measured spectrofluorometrically as basal phase (A), and therefore, both phases in acini from different treatment groups were analyzed separately in panels C and D in addition to the basal $[Ca^{2+}]_i$ shown in panel B. Although basal $[Ca^{2+}]_i$ in acini from control pancreas (140 ± 5 nm) was not affected by bile duct ligation of up to 6 h (B, triangles) pancreatic duct ligation led to a continuous increase in basal $[Ca^{2+}]_i$ (B, filled circles). Conversely, the Ca^{2+} response during the peak (C) as well as the plateau phase (D) of the Ca^{2+} signal after acetylcholine stimulation was significantly reduced after pancreatic duct ligation. Note that Ca^{2+} response in C and D is shown as $\Delta[Ca^{2+}]_i = [Ca^{2+}]_i$ peak/plateau - $[Ca^{2+}]_i$ basal to correct for the different basal Ca^{2+} levels shown in panel B. Data represent the means \pm S.E., and asterisks indicate differences at the 5% level.

the groups or under any experimental conditions, and no differences between sham-operated, bile duct-ligated and pancreatic duct-ligated animals were found (data not shown), thus excluding significant necrosis or cellular leakage as a confounding factor for acinar cell impairment.

Single Cell Microfluorometry of Calcium Signaling—On the single cell level pancreatic acinar cells are known to respond with a characteristic $[Ca^{2+}]_i$ pattern in response to different concentrations of secretagogue, and pathological signaling patterns have been associated with the onset of pancreatitis (3, 27, 28). Submaximal concentrations of either acetylcholine or cholecystokinin evoke repetitive Ca^{2+} peaks, so-called Ca^{2+} oscillations, whereas maximal or supramaximal concentrations induce an initial peak that is followed by a subsequent plateau phase. When we stimulated single acinar cells from the pancreas of control mice with submaximal concentrations of cholecystokinin (20 μ M) almost 90% of the cells responded with Ca^{2+} oscillations, whereas 4% responded with a peak/plateau Ca^{2+} pattern. After 4 h of pancreatic duct ligation the percentage of cells that responded to the submaximal 20 μ M cholecystokinin concentration with a peak/plateau Ca^{2+} -pattern increased to 10% (Fig. 7A). The percentage of cell that had no $[Ca^{2+}]_i$ response at all on the other hand increased from 4% in bile duct-ligated controls to 27% after pancreatic duct obstruction. The physiological pattern of Ca^{2+} oscillations that predominated in most cells (\sim 90%) from control pancreas was found in only 63% of cells after ligation of the pancreatic duct (Fig. 7A).

When we studied the frequency and amplitude of Ca^{2+} oscillations by single cell microfluorometry we confirmed that individual resting $[Ca^{2+}]_i$ levels were indeed increased after mouse pancreatic duct ligation (to 95 ± 5 nm versus 76 ± 5 nm in bile duct ligation controls). In terms of Ca^{2+} oscillations pancreatic duct ligation shifted the signaling pattern toward

lower frequencies and lower amplitudes. Although the mean period of an oscillation was 76 ± 3 s (oscillatory frequency 0.79/min) in controls, it increased to 127 ± 10 s (frequency 0.47/min) after 4 h of pancreatic duct obstruction. Not only was the percentage of cells in the lower frequency band substantially increased (Fig. 7B), but also the amplitude of individual oscillations decreased from a mean of 491 ± 37 nm to a mean of 459 ± 50 nm after pancreatic duct ligation.

Transmembranous Calcium Fluxes—The fact that the secretagogue-stimulated $[Ca^{2+}]_i$ plateau phase as well as the frequency of Ca^{2+} oscillations is affected after pancreatic duct obstruction could be explained by changes in the calcium influx pathway (26). We, therefore, performed calcium influx experiments in which we replaced Ca^{2+} in acinar cell perfusion medium with manganese. In unstimulated control cells Ca^{2+} substitution by Mn^{2+} resulted in a basal decrease of the fura-2 signal at 360 nm, which reflects the leak influx of Mn^{2+} . This basal rate of Mn^{2+} entry was comparable in acinar cell from control animals (bile duct ligation) and in those after pancreatic duct ligation (Fig. 8A). In contrast, in cells after pancreatic duct ligation the Mn^{2+} entry in response to acetylcholine stimulation, which reflects Mn^{2+} influx via a receptor-operated Ca^{2+} channel, was reduced to \sim 65% that found in controls (Fig. 8B).

Effect of Intracellular Calcium Chelation—The association of pathological calcium-signaling patterns with premature digestive protease activation and the onset of duct ligation-induced pancreatitis would predict that an interference with calcium signaling would prevent or ameliorate the experimental disease course. To test whether a causal relation exists between calcium signaling and the onset of duct ligation-induced pancreatitis, we treated animals *in vivo* with the AM ester of the calcium chelator BAPTA. This compound has been shown to bind intracellular calcium with high affinity in pancreatic aci-

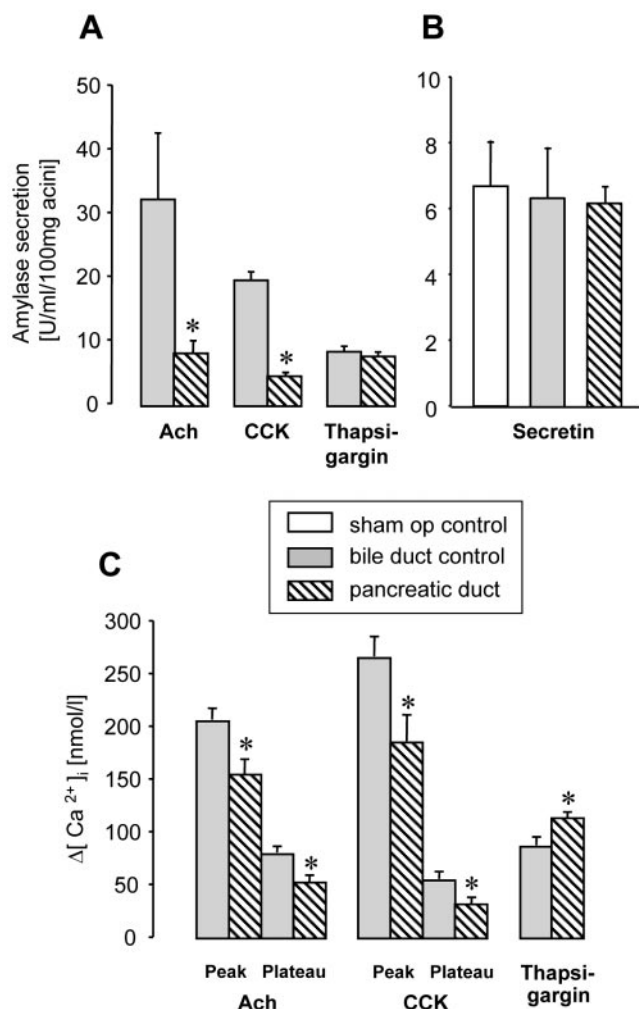


FIG. 6. Effect of different calcium-mobilizing agents on Ca^{2+} transients and acinar cell amylase secretion after pancreatic and bile duct ligation. Pancreatic acini from rat pancreas were prepared by collagenase after 4 h of either sham operation (*white bars*), bile duct ligation (*gray bars*), or pancreatic duct ligation (*hatched bars*). In *panel A* amylase secretion from acini in response to Ach (10^{-7} mol liter $^{-1}$), CCK (10^{-8} mol liter $^{-1}$), and the ATPase inhibitor thapsigargin (10^{-6} mol liter $^{-1}$) is shown, and in *panel C* the corresponding peak and plateau of $[Ca^{2+}]_i$ are indicated for the respective secretagogues. *Panel B* shows the cAMP-dependent and secretin-stimulated ($0.1 \mu M$) amylase secretion. In contrast to the biphasic Ca^{2+} response after Ach and CCK, thapsigargin induced only a monophasic Ca^{2+} transient. Although the Ach- and CCK-stimulated Ca^{2+} response as well as amylase secretion were greatly reduced after pancreatic duct obstruction, the thapsigargin-induced amylase secretion remained unchanged, and the according Ca^{2+} response was even somewhat increased. No difference between the groups in secretin-stimulated amylase secretion was found (*panel B*). Data represent the means \pm S.E., and asterisks indicate differences at the 5% level. U, unit(s).

nar cells (3). In mice that had received two intraperitoneal injections of BAPTA-AM before pancreatic duct ligation at a non-toxic concentration of $10 \mu g/kg$, the pancreatitis-induced rise of serum amylase and lipase as well as the premature activation of trypsinogen in the pancreas were reduced by more than 50% (Fig. 9, A–C). Higher concentrations of BAPTA-AM that could potentially have prevented pancreatitis completely could not be employed because of unacceptable systemic toxicity.

DISCUSSION

Under physiological resting conditions most cell types, including the acinar cells of the exocrine pancreas, maintain a Ca^{2+} gradient across the plasma membrane with low intracel-

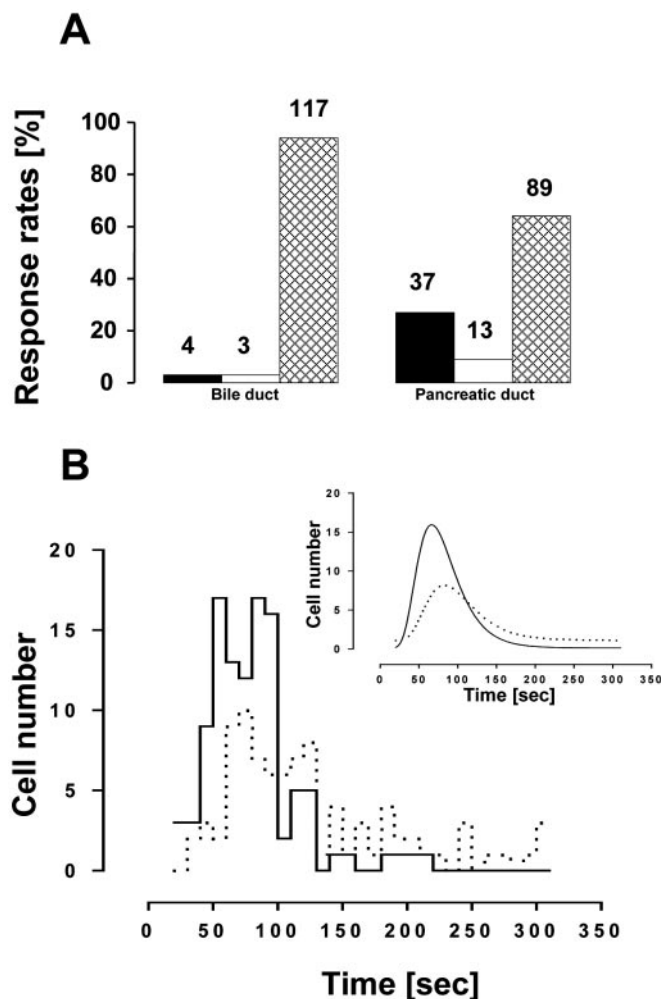


FIG. 7. Single cell $[Ca^{2+}]_i$ changes after pancreatic and bile duct ligation. Isolated acini from mouse pancreas were prepared by collagenase digestion 4 h after ligation of the pancreatic or bile duct in mice. Stimulation with submaximal concentrations of CCK ($20 \text{ pmol liter}^{-1}$) elicited rhythmic Ca^{2+} oscillations (*cross-hatched bars*) in 96% of cells, a peak/plateau pattern (*white bars*) in 2%, and no response (*black bars*) in 2% of cells. After pancreatic duct ligation (*right set of columns*), the number of cell without Ca^{2+} response rose to 24%, that with a peak/plateau pattern rose to 10%, and the proportion of cells with physiological Ca^{2+} oscillations declined to 62%. The numbers above the respective columns indicate the total number of cells in each group. In *panel B* the oscillation patterns in single acinar cells are shown after 4 h of bile duct ligation (*straight line*) or pancreatic duct ligation (*dotted line*). Oscillation periods are indicated on the horizontal axis in 10-s intervals, and the number of cells with oscillations lasting for the respective period was blotted on the vertical axis. The mean duration of oscillations was 75 s for acinar cells after bile duct ligation (oscillation frequency of $\sim 0.8/\text{min}$), whereas it was 130 s ($\sim 0.5/\text{min}$) after pancreatic duct ligation. The inset in *panel B* represents the regression curves derived from the data below in *B*.

lular (nanomolar range) facing high extracellular (millimolar range) Ca^{2+} concentrations. A rapid Ca^{2+} release from intracellular stores in response to external and internal stimuli is used by many of these cells as a signaling mechanism that regulates such diverse biological events as growth and proliferation, locomotion and contraction, and the regulated secretion of exportable proteins. A disturbance of the cellular Ca^{2+} balance and gradient has long been suspected to play a role in the pathophysiology of acute pancreatitis, because elevated extracellular Ca^{2+} concentrations represent a distinct risk factor for developing the disease. This association has been established for endocrine disorders associated with hypercalcemia (27) and has also been reported for patients who develop pan-

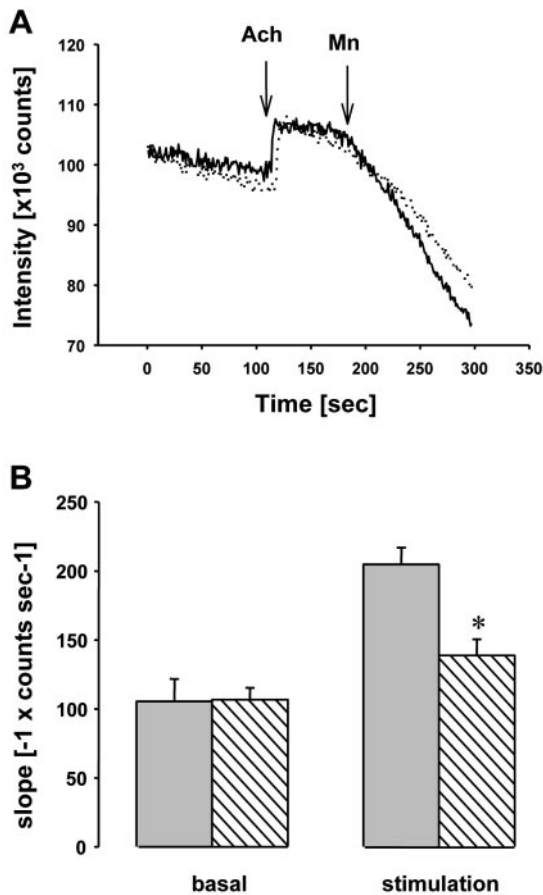


FIG. 8. Effect of pancreatic and bile duct ligation on the calcium influx pathway. The representative recordings at 360 nm (the isosbestic line of fura-2) in panel A gives an example of the manganese influx measurements. After stimulation of acinar cells with Ach (10^{-7} mol liter $^{-1}$), a small signal increase is followed by a precipitous decline at the time when Mn^{2+} is added, which indicates quenching of the dye by Mn^{2+} influx into the cell via the receptor-operated calcium channel. This Mn^{2+} influx is an indicator of Ca^{2+} influx and is reduced in acini from pancreatic duct-ligated animals (dotted line) in comparison to those from bile duct-ligated animals (continuous line). The histograms in panel B summarize the results from 35 experiments and indicate that Mn^{2+} quenching of fura-2 in unstimulated acinar cells (basal) was identical in acini from bile duct-ligated (gray bars) and pancreatic duct-ligated (hatched bars) animals, which indicates an unchanged Ca^{2+} leak influx under resting conditions. Mn^{2+} influx after acetylcholine (10^{-7} mol liter $^{-1}$) stimulation on the other hand was found to be significantly reduced in acini after pancreatic duct ligation. Data represent the means \pm S.E., and asterisks indicate differences at the 5% level.

creatitis after open heart surgery because of the supraphysiological Ca^{2+} concentrations in the solutions used for extracorporeal circulation (28). In laboratory animals experimental hypercalcemia has been shown to either decrease the threshold level for the induction of pancreatitis or to induce morphological alterations that parallel those seen in pancreatitis (29, 30). In a model of experimental pancreatitis in which the disease induction is achieved by injection of supraphysiological secretagogue concentrations a progressive disruption of intracellular Ca^{2+} signaling was reported (1). Accordingly, it has been proposed that an elevation of acinar cell cytosolic-free ionized calcium represents the most probable common denominator for the onset of various clinical varieties of pancreatitis (31). Support for this hypothesis came from studies in which calcium chelators were found to prevent an intracellular activation of pancreatic digestive enzymes in isolated acini (3, 6, 32).

In the present study we have investigated the intracellular Ca^{2+} dynamics in acinar cells using a pancreatitis model that

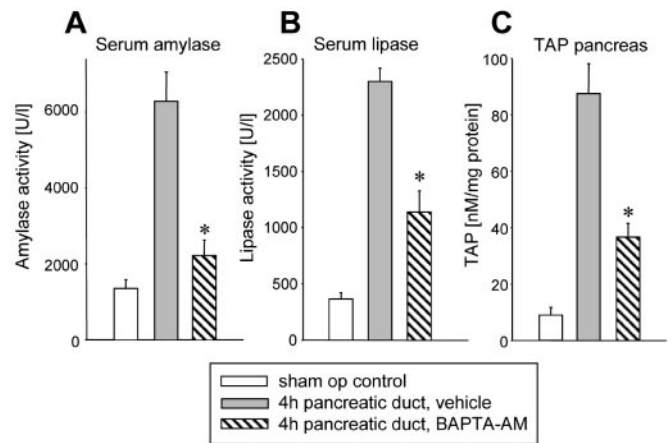


FIG. 9. Effect of the intracellular Ca^{2+} -chelator BAPTA-AM on intrapancreatic trypsinogen activation and serum pancreatic enzyme activities. NMRI mice underwent pancreatic duct ligation or sham operation (*sham op*) and were sacrificed after 4 h. Serum amylase activity (A), serum lipase activity (B), and TAP levels in pancreatic tissue homogenate (C) were measured as described under "Experimental Procedures." Animals with pancreatic duct ligation received 2 intraperitoneal injections (30 min before and at the time of laparotomy) of either BAPTA-AM (10 μ g/kg of body weight in 180 μ l of propylene glycol as vehicle hatched bars) or vehicle alone (gray bars). Treatment with the Ca^{2+} chelator BAPTA-AM reduced serum pancreatic enzyme activities as well as intrapancreatic trypsinogen activation significantly. Complete inhibition, which arguably could have been obtained with higher BAPTA-AM concentrations, was not achievable because of systemic toxic effects at higher doses of the chelator. Data represent the means \pm S.E., and asterisks indicate significant differences at the 5% level compared with vehicle-treated animals. U, unit(s).

is induced by pancreatic duct ligation, and we have chosen this approach for several reasons as follows. (a) The disease phenotype, although associated with premature intrapancreatic digestive enzyme activation, hyperamylasemia, pancreatic edema, and a systemic inflammatory response, is associated with only a moderate extent of acinar cell injury that does not preclude the investigation of signaling events in freshly isolated cells. (b) The mechanism of disease induction, surgical pancreatic duct ligation, does not involve a non-physiological stimulus that is inherently coupled to intracellular Ca^{2+} release like that in the secretagogue-induced pancreatitis models. (c) The triggering event of pancreatic duct obstruction represents, unlike supramaximal cholecystokinin stimulation, a common factor in the clinical disease variety of gallstone-induced pancreatitis (33).

We found that short term ligation of the pancreatic duct in the rat or mouse leads, in analogy to the common secretagogue-induced model of pancreatitis, to pancreatic edema, elevated serum pancreatic enzymes, a systemic inflammatory response, and premature intrapancreatic digestive zymogen activation. Using TAP levels as a measure of comparison, intrapancreatic trypsinogen activation is \sim 30% higher in the duct obstruction model versus the secretagogue model, although in neither model trypsinogen activation exceeds \sim 1% of the total cellular trypsinogen content. On the ultrastructural level duct ligation-induced pancreatitis is of considerably less severity than the secretagogue-induced model, and neither involves the massive formation of cytoplasmic vacuoles nor an impairment of the actin microfilament web along the acinar lumen. The pathological consequences of an F-actin redistribution from the basal plasma membrane of acinar cells observed after pancreatic duct ligation is harder to determine at present but does not seem to involve the fusion/fission events involved in zymogen granule exocytosis.

In terms of acinar cell function after pancreatic duct obstruc-

tion we found a profound disturbance of the intracellular Ca^{2+} homeostasis under both basal and hormone-stimulated conditions, which suggests a progressive disruption of Ca^{2+} -dependent signaling processes. These included a progressively increased basal $[\text{Ca}^{2+}]_i$ level that is generally regarded as an imbalance between Ca^{2+} influx, Ca^{2+} release from intracellular stores, and active Ca^{2+} export from the cytosol. Such an impaired cellular capacity to maintain the Ca^{2+} gradient across the plasma membrane has previously been identified as a common pathophysiological characteristic of vascular hypertension (34, 35), malignant tumor growth (36, 37), and cell damage in response to toxins (38). It has also been observed in the secretagogue-induced model of acute pancreatitis (1, 39). Our manganese influx studies suggest that the increased $[\text{Ca}^{2+}]_i$ is not caused by an impaired integrity of the plasma membrane because the basal or "leak" manganese influx remained unchanged after pancreatic duct ligation. We therefore suggest that an impairment of the calcium pumps accounts for the increased basal $[\text{Ca}^{2+}]_i$ level and non-physiological gradient. One mechanism that is likely to be involved in this process is the generation of oxygen radical species, which are not only released in abundance by acinar cells during pancreatitis but are also known to inhibit calcium pumps (40, 41, 42).

Another characteristic of pancreatic duct obstruction in our study was the rapidly decreasing Ca^{2+} response of pancreatic acinar cells to stimulation with acetylcholine and cholecystokinin. These results further indicate a differential intracellular calcium sequestration because the mobilization of calcium from acetylcholine and cholecystokinin-sensitive stores was greatly impaired, whereas neither the amylase secretion nor the Ca^{2+} release in response to thapsigargin was negatively affected. This suggests that, in addition to raised basal calcium levels, a preferential refilling of thapsigargin-sensitive stores as opposed to Ach- or CCK-sensitive stores, is a consequence of short term pancreatic duct obstruction. As previously demonstrated by Cancela *et al.* (43), Ach and CCK address through different mechanisms a common Ca^{2+} oscillatory unit that most probably consists of closely clustered inositol 1,4,5-trisphosphate and ryanodine channels (43). The increased number of cells after pancreatic duct ligation that responded with an irregular Ca^{2+} -signaling pattern (*i.e.* peak plateau instead of oscillations) allows for the possibility that this common oscillatory element is disrupted or impaired. The fact that both the maximal peak Ca^{2+} response after secretagogue stimulation as well as the sustained plateau phase of $[\text{Ca}^{2+}]_i$ were affected by duct ligation indicates that not only the rapid release of Ca^{2+} from intracellular stores but also the Ca^{2+} influx across the plasma membrane was impaired. An involvement of the latter event was further confirmed by our manganese experiments, which clearly demonstrated a reduced Ca^{2+} influx after duct ligation and, thus, provided an explanation for the reduced refilling of intracellular Ca^{2+} stores.

Finally, the observation that neither the calcium release nor amylase secretion in response to the ATPase inhibitor thapsigargin was reduced after pancreatic duct ligation nor that the enzyme secretion elicited via cAMP-dependent and secretin-stimulated pathways was impaired indicates that the secretory machinery required for enzyme exocytosis, which includes the fusion/fission events between secretory vesicles and the apical plasma membrane, were not disturbed by pancreatic duct obstruction. Taken together these data further refute the hypothesis that the secretory impairment after pancreatic duct obstruction is solely the result of a mechanical blockade of fluid secretion (12).

All the above data would support the conclusion that pancreatic duct obstruction is paralleled by very early and charac-

teristic changes in intracellular Ca^{2+} signaling but provide no direct evidence that irregular Ca^{2+} -signaling patterns are involved in the onset of the disease. When we used an intracellular Ca^{2+} chelator to interfere with intrapancreatic Ca^{2+} signaling we found that two characteristic parameters of early duct obstruction-induced pancreatitis, specifically elevated serum pancreatic enzyme levels and premature zymogen activation in the pancreas, were significantly reduced *in vivo*. This indicates that Ca^{2+} -signaling alterations are directly involved in the onset of experimental pancreatitis and provide the first direct *in vivo* evidence for this causal relation.

We conclude that in a model system that mimics the pathophysiological events involved in the onset of gallstone-induced pancreatitis we found that the Ca^{2+} signaling in isolated pancreatic acinar cells is markedly disturbed, that an increased resting $[\text{Ca}^{2+}]_i$ is not only paralleled by irregular Ca^{2+} responses to secretagogue stimulation but also by a reduced frequency and amplitude of Ca^{2+} oscillation as well as a decreased capacitative Ca^{2+} influx across the acinar cell membrane. These characteristic changes in intracellular Ca^{2+} signaling have been associated with and are indeed paralleled by a blockage of digestive enzyme secretion and premature digestive protease activation in the pancreas. They may, therefore, provide the first insight on the cellular level by what underlying mechanisms gallstone-induced pancreatitis is triggered. By systemic administration of the intracellular Ca^{2+} chelator BAPTA-AM, a novel approach to interfere with intrapancreatic Ca^{2+} signaling *in vivo*, we could demonstrate for the first time that $[\text{Ca}^{2+}]_i$ is indeed a critical mediator in the initiating phase of a clinically relevant model of acute pancreatitis.

Acknowledgment—We thank U. Breite for expert technical assistance.

REFERENCES

1. Ward, J. B., Sutton, R., Jenkins, S. A., and Petersen, O. H. (1996) *Gastroenterology* **111**, 481–491
2. Hofbauer, B., Saluja, A. K., Lerch, M. M., Bhagat, L., Bhatia, M., Lee, H. S., Frossard, J. L., Adler, G., and Steer, M. L. (1998) *Am. J. Physiol.* **275**, G352–G362
3. Krüger, B., Albrecht, E., and Lerch, M. M. (2000) *Am. J. Pathol.* **157**, 43–50
4. Grady, T., MahMoud, M., Otani, T., Rhee, S., Lerch, M. M., and Gorelick, F. S. (1998) *Am. J. Physiol.* **275**, G1010–G1017
5. Lerch, M. M., and Gorelick, F. S. (2000) *Med. Clin. N. Am.* **84**, 549–563
6. Raraty, M., Ward, J., Erdemli, G., Vaillant, C., Neoptolemos, J. P., Sutton, R., and Petersen, O. H. (2000) *Proc. Natl. Acad. Sci. U. S. A.* **97**, 13126–13131
7. Lerch, M. M., Saluja, A., Rünzi, M., Dawra, R., Saluja, M., and Steer, M. L. (1993) *Gastroenterology* **104**, 853–861
8. Acosta, J. M., Rubio Galli, O. M., Rossi, R., Chinellato, A. V., and Pellegrini, C. A. (1997) *J. Am. Coll. Surg.* **184**, 499–505
9. Lerch, M. M., Weidenbach, H., Hernandez, C. A., Preclik, G., and Adler, G. (1994) *Gut* **35**, 1501–1503
10. Hernandez, C. A., and Lerch, M. M. (1993) *Lancet* **341**, 1371–1373
11. Banks, P. A. (1998) in *Sleisinger and Fortran's Gastrointestinal and Liver Diseases* (Feldman, M., Scharschmidt, B. F., and Sleisinger, M. H., eds) 6th Ed., pp. 809–838, W. B. Saunders Co., Philadelphia
12. Isenman, L. D., and Rothman, S. S. (1979) *Science* **204**, 1212–1215
13. Opie, E. L. (1901) *Bull. Johns Hopkins Hosp.* **12**, 182–188
14. Mizutani, S., Miyata, M., Izukura, M., Tanaka, Y., and Matsuda, H. (1995) *Pancreas* **10**, 194–199
15. Senninger, N., Moody, F. G., Coelho, J. C., and Van Buren, D. H. (1986) *Surgery* **99**, 688–693
16. Schleicher, C., Baas, J. C., Elser, H., and Senninger, N. (2001) *Ann. Surg.* **233**, 528–536
17. Williams, J. A., Korc, M., and Dormer, R. L. (1978) *Am. J. Physiol.* **235**, 517–524
18. Lerch, M. M., Saluja, A. K., Dawra, R., Saluja, M., and Steer, M. L. (1993) *Gastroenterology* **104**, 1768–1779
19. Rinderknecht, J., and Marbach, E. P. (1970) *Clin. Chim. Acta* **29**, 107–110
20. Matthews, E. K., Petersen, O. H., and Williams, J. A. (1973) *J. Physiol.* **234**, 689–701
21. Neoptolemos J. P., Kemppainen E. A., Mayer J. M., Fitzpatrick J. M., Raraty M. G., Slavin J., Beger H. G., Hietaranta A. J., and Puolakkainen P. A. (2000) *Lancet* **355**, 1955–1960
22. Karanjia, N. D., Widdison, A. L., Jehanli, A., Hermon-Taylor, J., and Reber, H. A. (1993) *Pancreas* **8**, 189–195
23. Halangk, W., Lerch, M. M., Brandt-Nedele, B., Roth, W., Ruthenbuenger, M., Reinheckel, T., Domschke, W., Lippert, H., Peters, C., and Deussing, J. (2002) *J. Clin. Invest.* **106**, 773–781
24. Lerch, M. M., Saluja, A. K., Rünzi, M., Dawra, R., and Steer, M. L. (1995) *J. Clin. Invest.* **95**, 2222–2231

25. Gryniewicz, G., Poenie, M., and Tsien, R. Y. (1985) *J. Biol. Chem.* **260**, 3440–3450
26. Mooren, F. C., Turi, S., Gunzel, D., Schlue, W. R., Domschke, W., Singh, J., and Lerch, M. M. (2001) *FASEB J.* **15**, 659–672
27. Mithofer, K., Fernandez-del Castillo, C., Frick, T. W., Lewandrowski, K. B., Rattner, D. W., and Warshaw, A. L. (1995) *Gastroenterology* **109**, 239–246
28. Fernandez-del Castillo, C., Harringer, W., Warshaw, A. L., Vlahakes, G. J., Koski, G., Zaslavsky, A. M., and Rattner, D. W. (1991) *N. Engl. J. Med.* **325**, 382–387
29. Zhou, W., Shen, F., Miller, J. E., Han, Q., and Olson, M. S. (1996) *J. Surg. Res.* **60**, 147–155
30. Frick, T. W., Fernandez-del Castillo, C., and Bimmler, D., Warshaw, A. L. (1997) *Gut* **41**, 339–343
31. Ward, J. B., Peterson, O. H., Jenkins, S. A., and Sutton, R. (1995) *Lancet* **346**, 1016–1019
32. Saluja, A. K., Bhagat, L., Lee, H. S., Bhatia, M., Frossard, J. L., and Steer, M. L. (1999) *Am. J. Physiol.* **276**, G835–G842
33. Lerch, M. M., and Adler, G. (1993) *Curr. Opin. Gastroenterol.* **9**, 752–759
34. Blaustein, M. P. (1993) *Am. J. Physiol.* **264**, C1367–C1387
35. Resnick, L. (1999) *Prog. Cardiovasc. Dis.* **42**, 1–22
36. Poenie, M., Alderton, J., Tsien, R. Y., and Steinhardt, R. A. (1985) *Nature* **315**, 147–149
37. Alessandro, R., Masiero, L., Liotta, L. A., and Kohn, E. C. (1996) *In Vivo (Athens)* **10**, 153–160
38. Hameed, A., Olsen, K. J., Lee, M. K., Lichtenheld, M. G., and Podack, E. R. (1989) *J. Exp. Med.* **169**, 765–777
39. Bragado, M. J., San Roman, J. I., Gonzalez, A., Garcia, L. J., Lopez, M. A., and Calvo, J. J. (1996) *Clin. Sci. (Lond.)* **91**, 365–369
40. Zhao, B., Dierichs, R., Miller, F. N., and Dean, W. L. (1996) *Cell Calcium* **19**, 453–458
41. Schoenberg, M. H., Birk, D., and Beger, H. G. (1995) *Am. J. Clin. Nutr.* **62**, Suppl. 6, 1306–1314
42. Reinheckel, T., Prause, J., Nedelev, B., Augustin, W., Schulz, H. U., Lippert, H., and Halangk, W. (1999) *Digestion* **60**, 56–62
43. Cancela, J. M., Gerasimenko, O. V., Gerasimenko, J. V., Tepikin, A. V., and Petersen, O. H. (2000) *EMBO J.* **19**, 2549–2557